Current Biology 22, 397–402, March 6, 2012 ©2012 Elsevier Ltd All rights reserved DOI 10.1016/j.cub.2012.01.022

Report

Cholinergic Enhancement of Visual Attention and Neural Oscillations in the Human Brain

Markus Bauer,[1,2,*] Christian Kluge,[1,2,3] Dominik Bach,[1] David Bradbury,[1] Hans Jochen Heinze,[3] Raymond J. Dolan,[1] and Jon Driver[1,2]
[1]Wellcome Trust Centre for Neuroimaging, University College London, London WC1N3BG, UK
[2]UCL Institute of Cognitive Neuroscience, University College London, London WC1N3AR, UK
[3]Otto-von-Guericke-Universität Magdeburg, 39120 Magdeburg, Germany

Summary

Cognitive processes such as visual perception and selective attention induce specific patterns of brain oscillations [1–6]. The neurochemical bases of these spectral changes in neural activity are largely unknown, but neuromodulators are thought to regulate processing [7–9]. The cholinergic system is linked to attentional function in vivo [10–13], whereas separate in vitro studies show that cholinergic agonists induce high-frequency oscillations in slice preparations [14–16]. This has led to theoretical proposals [17–19] that cholinergic enhancement of visual attention might operate via gamma oscillations in visual cortex, although low-frequency alpha/beta modulation may also play a key role. Here we used MEG to record cortical oscillations in the context of administration of a cholinergic agonist (physostigmine) during a spatial visual attention task in humans. This cholinergic agonist enhanced spatial attention effects on low-frequency alpha/beta oscillations in visual cortex, an effect correlating with a drug-induced speeding of performance. By contrast, the cholinergic agonist did not alter high-frequency gamma oscillations in visual cortex. Thus, our findings show that cholinergic neuromodulation enhances attentional selection via an impact on oscillatory synchrony in visual cortex, for low rather than high frequencies. We discuss this dissociation between high- and low-frequency oscillations in relation to proposals that lower-frequency oscillations are generated by feedback pathways within visual cortex [20, 21].

Results

Neural processing of sensory signals originating from an attended location is thought to be enhanced by changes in oscillatory neural activity. Low-frequency alpha and beta oscillations in attended neuronal representations can be suppressed even before an expected stimulus appears (and enhanced for unattended) [5, 6]. This is thought to reflect up- and downregulation in the excitability of relevant neuronal populations [22]. Conversely, stimulus induced high-frequency gamma oscillations for attended neuronal representation are enhanced [1–4] and this is thought to increase their efficacy in driving postsynaptic neurons engendering privileged access to further processing stages [1, 23]. As for oscillations in general, the neurochemical pathways supporting these spectral changes are unknown but theoretical proposals suggest that an enhancement in high-frequency gamma oscillations is driven by cholinergic activity [17–19]. However, alpha oscillations are also known to be influenced by cholinergic neuromodulation [24–27].

Here we tested the impact of a cholinergic pharmacological intervention on brain oscillations during an attentional task in humans. Specifically, we recorded magnetoencephalography (MEG) while participants performed a spatial visual attention task (Figure 1), either under treatment with physostigmine [10, 11] as a cholinergic agonist or under placebo.

We recruited 16 participants who underwent both drug and placebo sessions (counterbalanced order) during this task. A central precue at trial start indicated which hemifield should be attended for a subsequently presented bilateral pair of gratings (see Figures 1B and 1C). The task was to discriminate orientation (clockwise or anticlockwise tilt relative to diagonal, titrated to yield ~90% accuracy) for the attended hemifield on each trial.

Under physostigmine, performance was faster than placebo (mean 779.8 ms versus 819.2 ms, mean speeding of 39.4 ms) without accuracy cost (mean 90% correct under physostigmine, 89% for placebo, n.s.). This difference was significant for reaction time (RT, $t = -1.84$, $p < 0.05$), when the order of drug and placebo was taken into account, as well as for inverse efficiency (combining RT and accuracy into a single value [28], $t = -2.52$, $p < 0.05$), and for the latter this was significant also without taking the order-effect into account ($t = -1.97$, $p < 0.05$). Thus, the drug improved performance, extending previous demonstrations that cholinergic enhancement can improve attentional processing.

We performed a time-frequency (t-f) analysis on MEG time courses projected onto the cortical surface, using a source-reconstruction method (see Supplemental Experimental Procedures) similar to previous studies [3, 4] to test the impact of the cholinergic agonist on well-known changes in oscillatory activity related to visuospatial attention. Directing attention to the left or right hemifield is known to suppress contralateral and/or increase ipsilateral alpha/beta activity [5, 6, 22], whereas gamma synchronization is enhanced [1–4] contralateral to the attended hemifield in visual cortex. Accordingly we tested for the expected symmetric attentional "hemispheric lateralization" effects in visual cortex (see Experimental Procedures for our formal symmetry constraint), then assessed any impact of physostigmine versus placebo upon either alpha/beta or gamma spatial attention effects.

Cholinergic Enhancement of Alpha/Beta Spatial Attention Effects

As expected [5, 6], alpha/beta hemispheric lateralization effects resulting from attended hemifield emerged in the preparatory cue period for occipital, parietal, and motor cortex (Figures 2A–2D), peaked around expected target onset, and then returned back to baseline levels. The novel result is that here alpha/beta spatial attention effects on visual cortex were enhanced by our cholinergic manipulation, being more pronounced under physostigmine than placebo

*Correspondence: markus.bauer@gmail.com

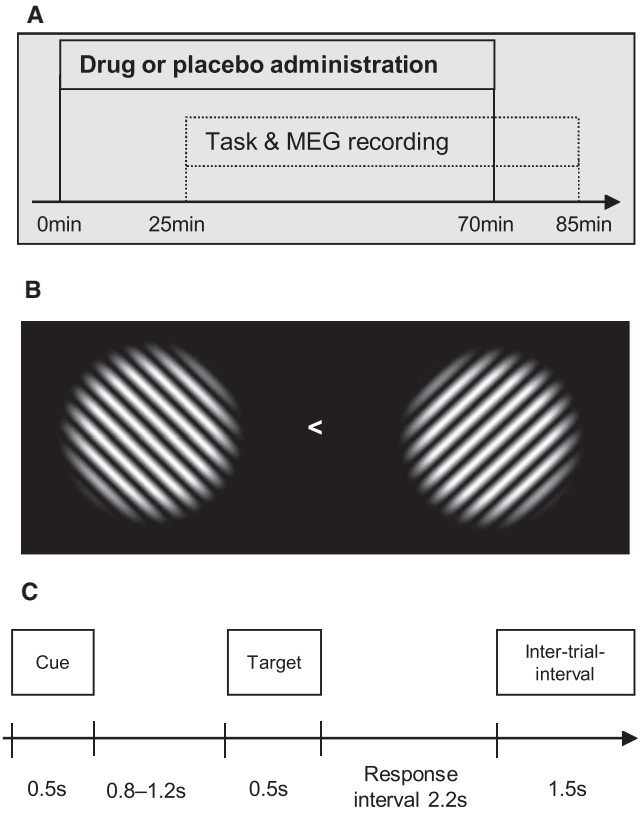

Figure 1. Experimental Timeline and Stimuli

(A) Physostigmine or placebo was administered intravenously starting 25 min prior to onset of the visuospatial attention task and concurrent MEG recording, then continuing until 15 min prior to end of experimental session.

(B) Each trial began with onset of a symbolic cue (right or left arrow, as shown) for 500 ms, indicating which hemifield to attend. Participants fixated the central cross throughout the remainder of the trial, which comprised a 0.8–1.2 s (rectangular distribution) cue-target interval, followed by presentation of bilateral gratings for 500 ms, with up to 2.2 s for participants to make the tilt judgement (clockwise or counterclockwise relative to diagonal) for the grating in the attended hemifield.

(C) Example display of bilateral gratings, spatial frequency 1.2 cycles/degree, circular window of 7 degrees, centered at 8 degrees eccentricity along the horizontal meridian.

(see Figures 2E and 2F for direct comparison, $p < 0.0001$, uncorrected). This cholinergic enhancement of alpha/beta spatial attention effects had a maximum in parieto-occipital cortex (see Table S1 for coordinates) and was evident both before and after stimulus onset. Because the parieto-occipital sulcus itself has been tightly linked to posterior alpha oscillations [29, 30] and even cholinergic neuromodulation [26, 27], we had a closer look at this region and placed a spatial filter in the left and right bank of the parieto-occipital sulcus. This revealed a clear maximum in a cholinergic enhancement effect on spatial attention in the poststimulus phase in the classical alpha band (peak frequency of 10 Hz, see Figure S1, $p < 0.005$). Notably, despite the fact that some of these effects were clearly in the poststimulus phase, the observed attentional lateralization and its enhancement by the cholinergic agonist was largely independent of stimulus-evoked components (see also [4]), as indicated by the fact that subtraction of the latter from individual trials did not change these results (Figure S1).

No Cholinergic Modulation of Gamma Attention Effects in Visual Cortex

Consistent with previous reports [1–4], we found lateralized effects due to attended hemifield on gamma activity for visual cortex ($p < 0.0001$, uncorrected), extending into lateral occipital and ventral occipito-temporal cortex; see Figure 3. These gamma spatial attention effects emerged rapidly after stimulus onset and then endured for ~500 ms. But note that these gamma attention effects were clearly *not* enhanced by physostigmine here, being highly reproducible in both the drug and placebo sessions (see Figure 3), with no significant difference ($p > 0.2$, was actually for slightly reduced gamma attentional effects under physostigmine). Likewise, stimulus-related visual gamma responses, due merely to onset of the visual gratings independent of attended hemifield, were also unaffected by physostigmine (see Figure S2). We note for completeness (and to show that gamma elsewhere could be affected) that there was a clear enhancement of a poststimulus-induced gamma-band response in frontal cortex ($p < 0.01$, uncorrected, see Figure S2). The impact of the drug on oscillations in early visual cortex was thus highly specific for the alpha/beta bands.

Brain-Behavior Relations Induced by the Cholinergic Agonist

Finally we turned to possible relations between the neurophysiological effects and performance effects of our cholinergic intervention. We correlated the participant-by-participant drug effect on inverse efficiency scores (combining response speed and accuracy) to each of the neurophysiological effects described above (and as depicted in Figures 2, 3, S1, and S2) for the t-f windows shown. Note that these t-f windows had been selected independent of behavior, based either on attentional contrast in agreement with the literature or the difference between drug and placebo (Figures S1 and S2). The only significant brain-behavior relation observed was between drug-related performance speeding and the drug-induced poststimulus alpha spatial attention effects in the parieto-occipital sulcus ($r = 0.65$, $p < 0.01$). Although the effect in the extended time-frequency window in the lateral parts of parieto-occipital cortex as shown in Figures 2E and 2F were not significantly related to the behavioral effects, the poststimulus aspect (0–200 ms) was significant here, too ($r = 0.52$, $p < 0.05$). Given the limitation of this correlation to the poststimulus period, we further investigated whether this effect might by itself depend on any stimulus-evoked components but also checked on general effects of alpha/beta power irrespective of spatial attention. To this end we subtracted the stimulus-evoked field from the spectrograms (as in Figure S1) and computed a partial correlation analysis removing any general effects of alpha/beta power. Figure S3 shows the scatterplot for this analysis and reveals that the partial correlation for alpha lateralization in the parieto-occipital sulcus increased to $r = 0.71$ ($p < 0.01$) but decreased for the lateral aspects of parieto-occipital cortex ($r = 0.41$, $p > 0.05$). Thus, the key impact of the cholinergic agonist was upon alpha/beta oscillations modulated top-down by spatial attention in visual cortex. By contrast, gamma oscillations in visual cortex were unaffected.

Discussion

Here we demonstrate via a causal intervention with a cholinergic agonist (physostigmine) that cholinergic neuromodulation augments the top-down impact of spatial attention on

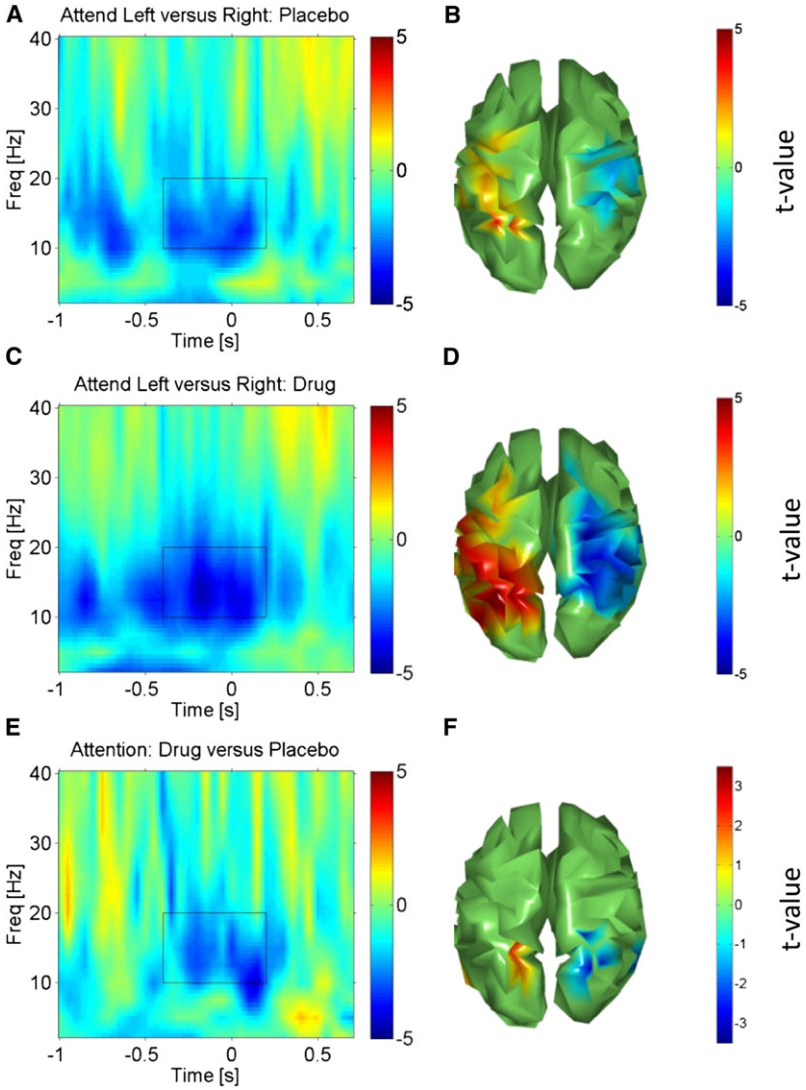

Figure 2. Spatial Attention and Alpha/Beta Oscillations

(A) Time-frequency (t-f) profile for effect of spatial attention in the placebo session for symmetric hemispheric lateralization effects of Attention Left minus Attention Right at low frequency oscillations. Time zero corresponds to target onset in this and all subsequent t-f plots, and the color bar indicates t values. The t-f plot combines analogous effects in the left and right hemisphere.

(B) The topography reveals suppressed/enhanced alpha/beta power (t-f window marked in A) in the hemisphere contralateral/ipsilateral to the attended hemifield, as expected (blue colors represent suppression, red enhancement).

(C and D) T-f profile for corresponding effect of spatial attention in the physostigmine condition, with topography shown in (D); note the enhanced effect compared with (A) and (B).

(E) T-f profile for the direct contrast of spatial attention effect in physostigmine minus placebo conditions, with topography shown in (F).

(F) The cholinergic enhancement is localized to parieto-occipital cortex, an area tightly linked to alpha oscillations (see also Figure S1 for closer investigation of the parieto-occipital sulcus). Topographies are thresholded at $p < 0.05$, uncorrected, but for symmetric voxel pairs (see Experimental Procedures).

oscillations in human visual cortex, specifically for low-frequency alpha/beta bands. Previous studies show that cholinergic agonists enhance the hemodynamic BOLD response [10, 11] to attended stimuli in visual cortex or spike-rates recorded invasively [13] in primary visual cortex but the studies had not examined oscillatory phenomena. Although our results show the same pattern of spatial attention effects as a previous MEG study on spatial attention [4]—contralateral suppression (or/and ispilateral enhancement) of alpha/beta oscillations and contralateral enhancement of gamma oscillations—we show that a cholinergic enhancement via physostigmine boosts attentional alpha/beta effects in human visual cortex (Figure 2) but did not impact gamma effects in visual cortex (Figure 3; see also Figure S2). Moreover, the cholinergic impact on alpha/beta spatial attention effects were correlated to a drug-induced improvement in performance (Figure 4), such that strong attentional lateralization coincided with more efficient task processing, whereas any potential drug effect on visual gamma phenomena did not show such a correlation. Our alpha/beta findings provide a new line of evidence for the emerging view that low-frequency oscillations in visual cortex (and sensory cortex more generally) play a key role in gating sensory processing [6, 22, 31].

The specific relation to the drug-enhanced performance speeding here indicates that the cholinergic impact on attentional alpha/beta effects is not merely epiphenomenal.

In contrast to the impact on alpha/beta attention effects, the robustly observed gamma effects resulting from attended hemifield in visual cortex were *not* modified by the drug. This is a surprising outcome for theories [17–19] proposing that cholinergic neuromodulation impacts attentional selection by modulating gamma synchrony in particular. But those proposals were probably influenced by findings from hippocampus [14–16] or auditory cortex of anesthetized animals [24, 25] after cholinergic manipulations, not from recordings in visual cortex during an attention task with a cholinergic intervention. Moreover, the one invasive study to date [32] that examined cholinergic modulation of visual cortex while recording oscillations (albeit in anesthetized cats, without any attention task) found no immediate effect on the visually driven gamma response, analogous to our results (Figure S2) for awake humans in a cognitive task that allowed us to document spatial attention effects also (Figure 3). Note that we did, however, find an enhanced gamma-band response (after grating onset) in right frontal cortex (Figure S2), a brain structure that is intimately involved in control of attention [33] although it did not correlate with the performance speeding here. Likewise, in rats, frontal gamma oscillations may also depend on cholinergic activation [34].

Our findings suggest that cholinergic enhancement affects oscillatory activity in specific frequency bands, but differentially for distinct brain regions. This may relate to differential distribution of cholinergic receptors [35] and/or regional differences in circuitry, e.g., laminar activation patterns. One potential explanation for this arises from recent monkey studies [20, 21]. These highlight that gamma synchrony in visual cortex

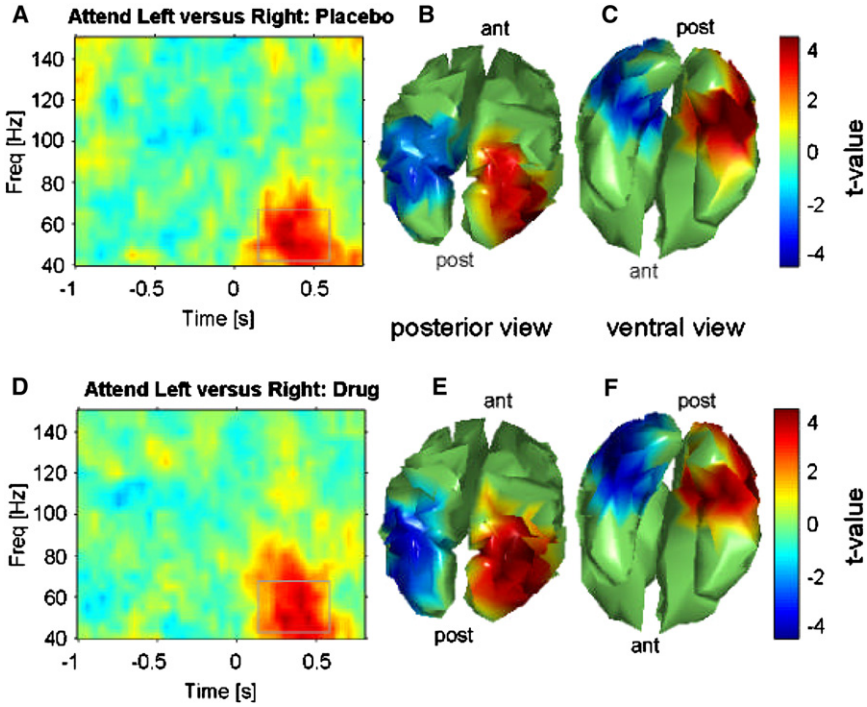

Figure 3. Spatial Attention and Gamma Oscillations

(A) Time-frequency profile for symmetric hemispheric lateralization effects of Attention Left minus Attention Right for high frequency oscillations under placebo.

(B and C) Topography of the high-frequency spatial attention effects under placebo for the time-frequency window marked in (A), shown in posterior view (B) or shown in ventral view (C), i.e., seen from below. Note that hot colors in the topographies indicate enhanced power contralateral to the attended hemifield, cold colors indicate reduced power ipsilateral to the attended hemifield.

(D–F) Corresponding data now shown under physostigmine. Note the high reproducibility of the spatial attention effects on gamma, identical under drug/placebo. As a consequence there was no significant enhancement of gamma attention effects by the drug (the nonsignificant trend was actually for slightly stronger gamma attention effects under placebo). All values plotted are t values for the contrast of Attention Left minus Attention Right.

Topographies are thresholded at $p < 0.05$, uncorrected, but for symmetric voxel pairs (see Experimental Procedures). See also Figure S2.

involves superficial (supragranular) feedforward layers, whereas alpha/beta synchrony involves predominantly the deeper (infragranular) feedback receiving layers. In the context of the present finding of cholinergic influence on alpha/beta, but not gamma, oscillations within human visual cortex, this raises the intriguing possibility of cholinergic enhancement primarily impacting feedback layers in the context of visual attention [35, 36]. Feedback influences are presumably key to top-down attentional influences. Although some proposals [37, 7] have emphasized enhanced bottom-up processing because of cholinergic modulation, other accounts propose cholinergic enhancement of attentional influences [8–13]. Our neurophysiological findings for human visual cortex document an example of the latter influence, yet, interestingly, we see this effect to extend well into the poststimulus period, suggesting a cholinergic impact on the interaction of bottom-up and top-down influences.

The drug used here, physostigmine, influences both nicotinic and muscarinic receptors [8], and it may be of interest to further distinguish the specific contributions of these in future work. Nevertheless, physostigmine has proven useful for studying the impact of the cholinergic system on neural processing in many previous studies [8–11] and is of particular interest as a drug applicable to humans. The importance of our results is that they provide the first evidence on how the cholinergic system modulates cortical oscillations, in the context of a visuospatial attention task, illustrating the power and potential of combining neuropharmacology with MEG [38, 39] and documenting the importance of low-frequency (alpha/beta) oscillations for visual attention.

Experimental Procedures

Participants

Sixteen healthy male volunteers (mean age 25.6 years, SD 5.7 years) participated after informed consent in accord with ethical clearance. Participants trained on the task and then performed two MEG sessions: one under drug, one with placebo in a double-blind crossover design.

Task

Two visual gratings appeared, one in each hemifield centered at 8 degrees eccentricity (see Figure 1). Each trial started with a precue (central arrow pointing left or right for 500 ms) followed by a cue-target interval (length varied uniformly and unpredictably from 800 to 1200 ms), then onset of bilateral gratings for 500 ms. The task was to judge a tilt-offset for the grating in the cued hemifield (clockwise or counterclockwise relative to the diagonal), as indicated by pressing a right or left button with the corresponding index finger as quickly and accurately as possible. The actual tilt offset was titrated to yield ~90% correct performance; see Supplemental Experimental Procedures for further details.

Procedure

For the pharmacological MEG sessions, the responsible physician administered either the drug (0.01 mg physostigmine per kg bodyweight and infusion time and 0.2 mg glycopyrrolate as a peripheral antagonist; see Supplemental Information and [10, 11]) or the equivalent amounts of a saline solution for placebo via an intravenous line.

Behavioral Data Analysis

We performed a regression analysis on the difference between drug and placebo in RT with drug/placebo session order as a covariate. The same analysis was performed for inverse-efficiency behavioral scores [36], which combine RT and accuracy as RT divided by proportion correct.

MEG Recording and Analysis

MEG data were recorded continuously with a CTF Omega system at sampling rate of 600 Hz and analysis was primarily implemented with FieldTrip [40], unless stated. Procedures for recording, preprocessing, and artifact treatment followed previous work closely [1] as further described in Supplemental Experimental Procedures. For source reconstruction, we used a single-shell forward model [41] that was derived from the cortical sheets of each participant by a nonlinear warp of their brain to the MNI brain via SPM8 [42]. We used a beamforming approach [43, 44] to project the sensor data onto a (spatially) downsampled cortical grid representation. We then performed a time frequency analysis of the time courses on source level. For low-frequency bands (2.5–40 Hz), a wavelet analysis was computed and for the high-frequency bands, a multitaper analysis was computed.

Analysis for Spatial Attention Effects

In order to minimize false positives, by design we implemented the following formal procedure to test here for symmetrically lateralized spatial attention

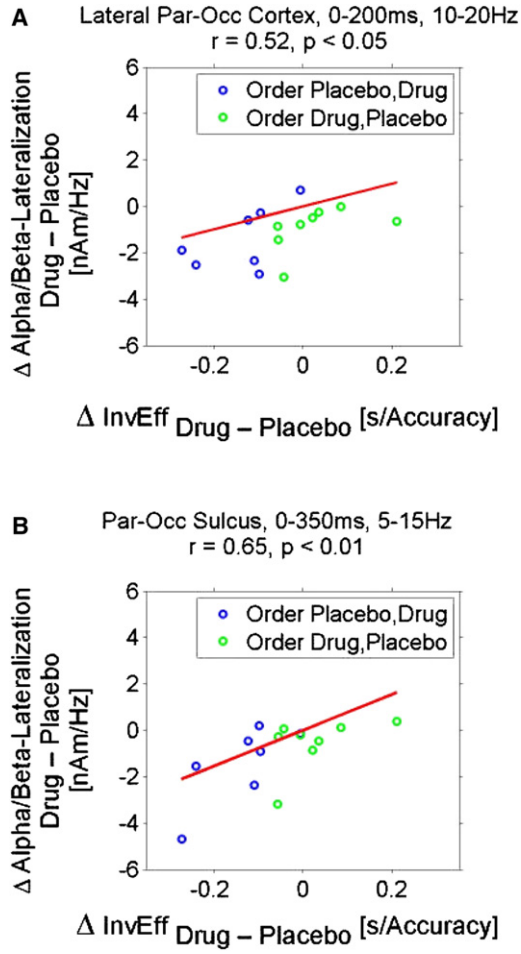

Figure 4. Brain-Behavior Relations

Scatterplots with regression lines showing significant correlation of drug impact on poststimulus alpha/beta spatial attention effects with inverse efficiency scores for parieto-occipital cortex (see Figures 2E, 2F, and S1).

(A) Correlation with the lateral parts of parieto-occipital cortex (Figure 2F, 10–20 Hz, 0–200 ms).

(B) Correlation with an ROI in the parieto-occipital sulcus (Figure S1), a structure tightly linked with alpha oscillations at the t-f window where the drug effect is maximal there (5–15 Hz, 0–350 ms).

Difference of attentional lateralization (Attention Left minus Attention Right) in power for right minus left hemispheres are shown on the *y* axis, differences of inverse efficiency is shown on the *x* axis. Each point gives difference scores for one participant, in blue the subjects where the drug session followed placebo and in green where drug preceded placebo. Negative values on the *x* and *y* axis indicate stronger effects in the expected direction (stronger hemispheric lateralization and faster processing for the physostigmine condition). Subjects for whom the drug was administered in the second session tend to have stronger effects. See also Figure S3.

effects. To test for the main effect of spatial attention, t tests were calculated for the difference between "Attend_Left" and "Attend_Right" for each grid point in the respective time-frequency windows. The symmetry constraint was operationalized by retaining only grid points that showed a significant difference ($p < 0.05$) in the above contrast (Attend_Left versus Attend_Right) *and* had a *corresponding grid point* for the reverse contrast (see Supplemental Experimental Procedures for further details). Subsequent tests for any drug modulation of attention effects also had the mirror symmetry constraint on paired t tests of attentional hemispheric lateralization.

Correlation of Physiological Measures with Behavior

We related the drug impact on inverse efficiency to the drug impact on those MEG results of interest already reported to avoid a blind search through the entire brain-time-frequency matrix.

Supplemental Information

Supplemental Information includes Supplemental Experimental Procedures, three figures, and one table and can be found with this article online at doi:10.1016/j.cub.2012.01.022.

Acknowledgments

This work was funded by the Wellcome Trust 087756/Z/08/Z. J.D. was a Royal Society Research Professor, M.B. had been funded by the Medical Research Council (G0500784), C.K. and H.J.H. were supported by Deutsche Forschungsgemeinschaft SFB 779, TP A2. The Wellcome Trust Centre for Neuroimaging is supported by core funding from the Wellcome Trust 091593/Z/10/Z.

Received: September 19, 2011
Revised: December 6, 2011
Accepted: January 11, 2012
Published online: February 2, 2012

References

1. Womelsdorf, T., and Fries, P. (2007). The role of neuronal synchronization in selective attention. Curr. Opin. Neurobiol. *17*, 154–160.
2. Fries, P., Reynolds, J.H., Rorie, A.E., and Desimone, R. (2001). Modulation of oscillatory neuronal synchronization by selective visual attention. Science *291*, 1560–1563.
3. Bauer, M., Oostenveld, R., Peeters, M., and Fries, P. (2006). Tactile spatial attention enhances gamma-band activity in somatosensory cortex and reduces low-frequency activity in parieto-occipital areas. J. Neurosci. *26*, 490–501.
4. Siegel, M., Donner, T.H., Oostenveld, R., Fries, P., and Engel, A.K. (2008). Neuronal synchronization along the dorsal visual pathway reflects the focus of spatial attention. Neuron *60*, 709–719.
5. Worden, M.S., Foxe, J.J., Wang, N., and Simpson, G.V. (2000). Anticipatory biasing of visuospatial attention indexed by retinotopically specific alpha-band electroencephalography increases over occipital cortex. J. Neurosci. *20*, RC63.
6. Haegens, S., Händel, B.F., and Jensen, O. (2011). Top-down controlled alpha band activity in somatosensory areas determines behavioral performance in a discrimination task. J. Neurosci. *31*, 5197–5204.
7. Yu, A.J., and Dayan, P. (2005). Uncertainty, neuromodulation, and attention. Neuron *46*, 681–692.
8. Hasselmo, M.E., and Sarter, M. (2011). Modes and models of forebrain cholinergic neuromodulation of cognition. Neuropsychopharmacology *36*, 52–73.
9. Bentley, P., Driver, J., and Dolan, R.J. (2011). Cholinergic modulation of cognition: insights from human pharmacological functional neuroimaging. Prog. Neurobiol. *94*, 360–388.
10. Furey, M.L., Pietrini, P., and Haxby, J.V. (2000). Cholinergic enhancement and increased selectivity of perceptual processing during working memory. Science *290*, 2315–2319.
11. Bentley, P., Vuilleumier, P., Thiel, C.M., Driver, J., and Dolan, R.J. (2003). Cholinergic enhancement modulates neural correlates of selective attention and emotional processing. Neuroimage *20*, 58–70.
12. Sarter, M., Hasselmo, M.E., Bruno, J.P., and Givens, B. (2005). Unraveling the attentional functions of cortical cholinergic inputs: interactions between signal-driven and cognitive modulation of signal detection. Brain Res. Brain Res. Rev. *48*, 98–111.
13. Herrero, J.L., Roberts, M.J., Delicato, L.S., Gieselmann, M.A., Dayan, P., and Thiele, A. (2008). Acetylcholine contributes through muscarinic receptors to attentional modulation in V1. Nature *454*, 1110–1114.
14. Traub, R.D., Bibbig, A., Fisahn, A., LeBeau, F.E., Whittington, M.A., and Buhl, E.H. (2000). A model of gamma-frequency network oscillations induced in the rat CA3 region by carbachol in vitro. Eur. J. Neurosci. *12*, 4093–4106.
15. Tiesinga, P.H., Fellous, J.M., José, J.V., and Sejnowski, T.J. (2001). Computational model of carbachol-induced delta, theta, and gamma oscillations in the hippocampus. Hippocampus *11*, 251–274.
16. Mann, E.O., Suckling, J.M., Hajos, N., Greenfield, S.A., and Paulsen, O. (2005). Perisomatic feedback inhibition underlies cholinergically induced fast network oscillations in the rat hippocampus in vitro. Neuron *45*, 105–117.

17. Börgers, C., Epstein, S., and Kopell, N.J. (2005). Background gamma rhythmicity and attention in cortical local circuits: a computational study. Proc. Natl. Acad. Sci. USA *102*, 7002–7007.
18. Börgers, C., Epstein, S., and Kopell, N.J. (2008). Gamma oscillations mediate stimulus competition and attentional selection in a cortical network model. Proc. Natl. Acad. Sci. USA *105*, 18023–18028.
19. Deco, G., and Thiele, A. (2009). Attention: oscillations and neuropharmacology. Eur. J. Neurosci. *30*, 347–354.
20. Buffalo, E.A., Fries, P., Landman, R., Liang, H., and Desimone, R. (2010). A backward progression of attentional effects in the ventral stream. Proc. Natl. Acad. Sci. USA *107*, 361–365.
21. Maier, A., Adams, G.K., Aura, C., and Leopold, D.A. (2010). Distinct superficial and deep laminar domains of activity in the visual cortex during rest and stimulation. Front Syst Neurosci *4*, 31.
22. Jensen, O., and Mazaheri, A. (2010). Shaping functional architecture by oscillatory alpha activity: gating by inhibition. Front Hum Neurosci *4*, 186.
23. Salinas, E., and Sejnowski, T.J. (2001). Correlated neuronal activity and the flow of neural information. Nat. Rev. Neurosci. *2*, 539–550.
24. Metherate, R., and Ashe, J.H. (1993). Nucleus basalis stimulation facilitates thalamocortical synaptic transmission in the rat auditory cortex. Synapse *14*, 132–143.
25. Metherate, R., Cox, C.L., and Ashe, J.H. (1992). Cellular bases of neocortical activation: modulation of neural oscillations by the nucleus basalis and endogenous acetylcholine. J. Neurosci. *12*, 4701–4711.
26. Osipova, D., Ahveninen, J., Kaakkola, S., Jääskeläinen, I.P., Huttunen, J., and Pekkonen, E. (2003). Effects of scopolamine on MEG spectral power and coherence in elderly subjects. Clin. Neurophysiol. *114*, 1902–1907.
27. Osipova, D., Ahveninen, J., Jensen, O., Ylikoski, A., and Pekkonen, E. (2005). Altered generation of spontaneous oscillations in Alzheimer's disease. Neuroimage *27*, 835–841.
28. Townsend, J.T., and Ashby, F.G. (1983). The Stochastic Modelling of Elementary Psychological Processes (Cambridge: Cambridge University Press).
29. Manshanden, I., De Munck, J.C., Simon, N.R., and Lopes da Silva, F.H. (2002). Source localization of MEG sleep spindles and the relation to sources of alpha band rhythms. Clin. Neurophysiol. *113*, 1937–1947.
30. Tuladhar, A.M., ter Huurne, N., Schoffelen, J.M., Maris, E., Oostenveld, R., and Jensen, O. (2007). Parieto-occipital sources account for the increase in alpha activity with working memory load. Hum. Brain Mapp. *28*, 785–792.
31. Romei, V., Gross, J., and Thut, G. (2010). On the role of prestimulus alpha rhythms over occipito-parietal areas in visual input regulation: correlation or causation? J. Neurosci. *30*, 8692–8697.
32. Rodriguez, R., Kallenbach, U., Singer, W., and Munk, M.H. (2004). Short- and long-term effects of cholinergic modulation on gamma oscillations and response synchronization in the visual cortex. J. Neurosci. *24*, 10369–10378.
33. Capotosto, P., Babiloni, C., Romani, G.L., and Corbetta, M. (2009). Frontoparietal cortex controls spatial attention through modulation of anticipatory alpha rhythms. J. Neurosci. *29*, 5863–5872.
34. Berntson, G.G., Shafi, R., and Sarter, M. (2002). Specific contributions of the basal forebrain corticopetal cholinergic system to electroencephalographic activity and sleep/waking behaviour. Eur. J. Neurosci. *16*, 2453–2461.
35. Disney, A.A., Domakonda, K.V., and Aoki, C. (2006). Differential expression of muscarinic acetylcholine receptors across excitatory and inhibitory cells in visual cortical areas V1 and V2 of the macaque monkey. J. Comp. Neurol. *499*, 49–63.
36. Deco, G., and Thiele, A. (2011). Cholinergic control of cortical network interactions enables feedback-mediated attentional modulation. Eur. J. Neurosci. *34*, 146–157.
37. Hasselmo, M.E., and Giocomo, L.M. (2006). Cholinergic modulation of cortical function. J. Mol. Neurosci. *30*, 133–135.
38. Jensen, O., Goel, P., Kopell, N., Pohja, M., Hari, R., and Ermentrout, B. (2005). On the human sensorimotor-cortex beta rhythm: sources and modeling. Neuroimage *26*, 347–355.
39. Muthukumaraswamy, S.D., Edden, R.A., Jones, D.K., Swettenham, J.B., and Singh, K.D. (2009). Resting GABA concentration predicts peak gamma frequency and fMRI amplitude in response to visual stimulation in humans. Proc. Natl. Acad. Sci. USA *106*, 8356–8361.
40. Oostenveld, R., Fries, P., Maris, E., and Schoffelen, J.M. (2011). FieldTrip: Open source software for advanced analysis of MEG, EEG, and invasive electrophysiological data. Comput. Intell. Neurosci. *2011*, 156869.
41. Nolte, G. (2003). The magnetic lead field theorem in the quasi-static approximation and its use for magnetoencephalography forward calculation in realistic volume conductors. Phys. Med. Biol. *48*, 3637–3652.
42. Litvak, V., Mattout, J., Kiebel, S., Phillips, C., Henson, R., Kilner, J., Barnes, G., Oostenveld, R., Daunizeau, J., Flandin, G., et al. (2011). EEG and MEG data analysis in SPM8. Comput. Intell. Neurosci. *2011*, 852961.
43. Gross, J., Kujala, J., Hamalainen, M., Timmermann, L., Schnitzler, A., and Salmelin, R. (2001). Dynamic imaging of coherent sources: Studying neural interactions in the human brain. Proc. Natl. Acad. Sci. USA *98*, 694–699.
44. Van Veen, B.D., van Drongelen, W., Yuchtman, M., and Suzuki, A. (1997). Localization of brain electrical activity via linearly constrained minimum variance spatial filtering. IEEE Trans. Biomed. Eng. *44*, 867–880.

Current Biology, Volume *22*

Supplemental Information

Cholinergic Enhancement of Visual Attention and Neural Oscillations in the Human Brain

Markus Bauer, Christian Kluge, Dominik Bach, David Bradbury, Hans Jochen Heinze, Raymond J. Dolan, and Jon Driver

Supplemental Inventory

Drug modulation of attention effect in parieto-occipital sulcus

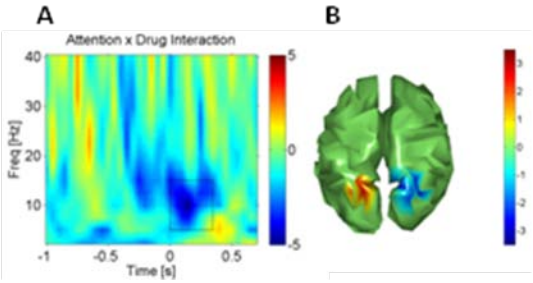

Attention: alpha/beta-band - Evoked field removed

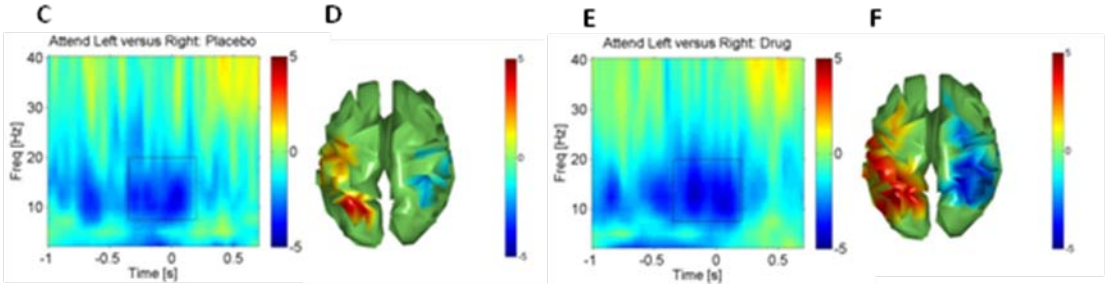

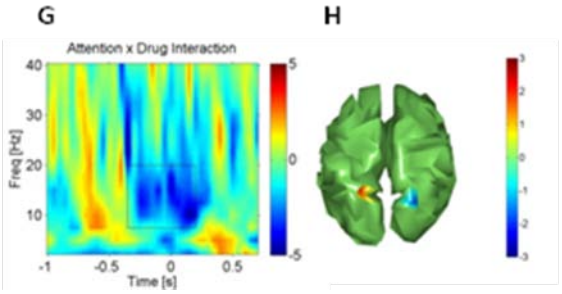

General alpha/beta event-related desynchronization **<u>independent of attentional state</u>**

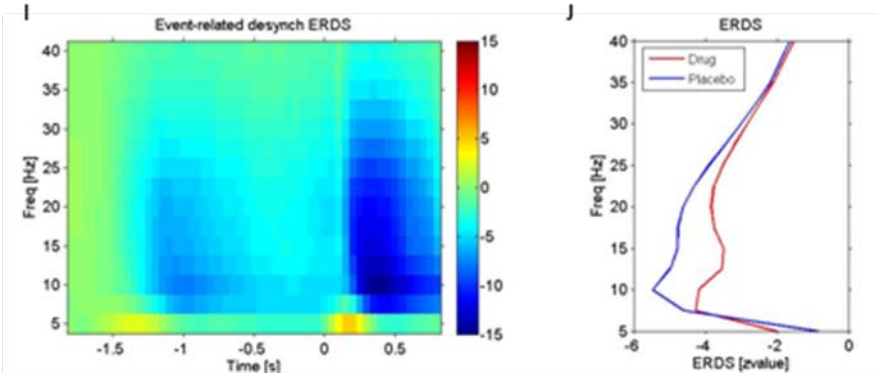

Figure S1 – Alpha/beta band in parieto-occipital cortex, **related to Figure 2**

(A-B): Cholinergic enhancement of attentional hemispheric lateralization as in Figure 3 E-F, but now for a ROI in the bank of the parieto-occipital sulcus: **(A)** The time-frequency (t-f) profile for

the drug related enhancement of the alpha/beta lateralization effect reveals a clear maximum in the post-stimulus phase, from approx. 0-300ms and a peak frequency of 10 Hz. **(B)** The topography shows the statistic of the effect in this window. Topography thresholded at $p<0.05$ with symmetry constraint.

(**C-H**) These panels are analogous to Figure 2 in the main manuscript but the evoked field was subtracted from individual trials to investigate whether the effect may have been driven by the frequency-representation of stimulus-locked evoked fields. The results confirm that the reported effects in the main manuscript are not driven by such evoked components. **(C)** The time-frequency (t-f) profile for the attention effect in the placebo condition. **(D)** The topography for the attention effect under placebo in the highlighted t-f window. **(E)** The time-frequency (t-f) profile for the attention effect in the physostigmine condition. **(F)** The topography for the attention effect under physostigmine in the highlighted t-f window. **(G)** The time-frequency (t-f) profile for the drug enhancement of the attention effect. **(H)** The topography for the drug enhancement of the attention effect in the highlighted t-f window (same as placebo). All plots show t-values and topographies thresholded at $p<0.05$, uncorrected but with symmetry constraint.

(I) Event related desynchronisation (locked to target onset) pooled over drug and placebo, independent of attentional state. **(J)** Frequency spectra in the time period from -350 to +200ms separately for drug and placebo. These figures show no clear separation for alpha- and beta-band.

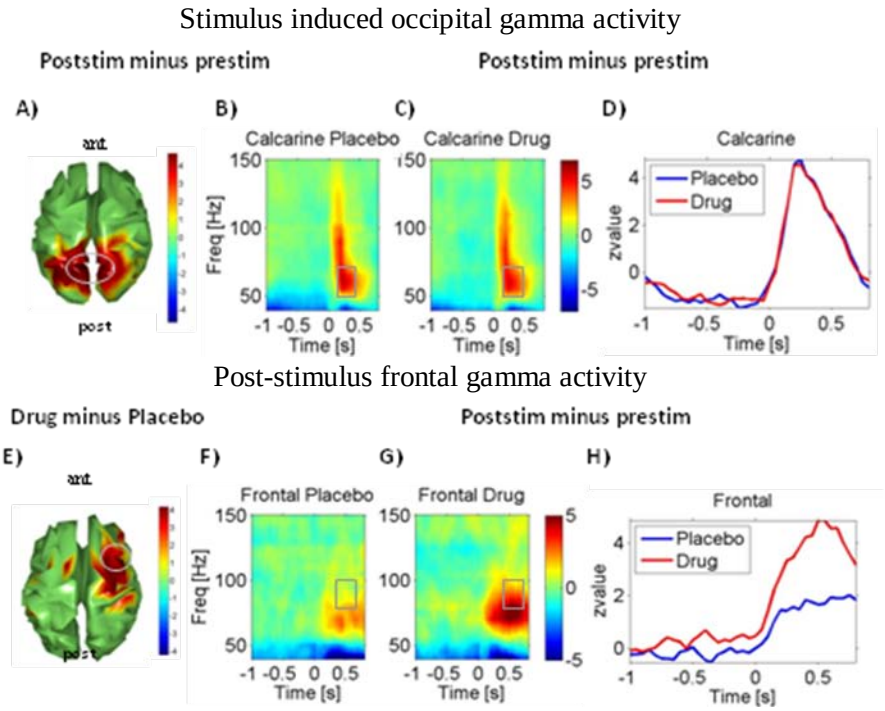

Figure S2 – Stimulus related gamma band activity, **related to Figure 3**

(A-D): Induced neural response to grating onset independent of attended side (i.e. pooled across attend left/right) for higher frequency bands. **(A)** Topography for stimulus-induced gamma increases regardless of drug (and of spatial attention), revealing robust posterior visual gamma responses in the period after visual target onset, corresponding to the window marked in the time-frequency profiles shown for early (peri-calcarine) visual cortex in **(B)** under placebo, and in **(C)** under physostigmine. Post=posterior aspect of brain, Ant=anterior. Note the very high reproducibility of the visually-induced gamma increase across placebo and drug conditions, Indeed there were no significant differences between visually-induced gamma under drug versus placebo, with the nonsigificant trend ($p>0.2$) actually being for slightly more gamma under placebo. **(D)** Shows timecourses of induced 50-70Hz gamma for these two conditions, again confirming the high reproducibility regardless of drug. Values plotted are z-values for post-vs pre-stimulus power. Topography thresholded at $p<0.01$.

(E-H): Induced gamma response as in (A), but now for the frontal areas that show an enhancement by the cholinergic agonist, in contrast to the unaffected gamma-band responses in visual cortex. **(E)** Topography for the statistical comparison between drug and placebo – showing an increased gamma-band response over (predominantly right) frontal cortex. **(F)** Time frequency profile of the response in area as marked in (E) under placebo, and in **(G)** under physostigmine. These are analogous to (B) and (C) but note here the clearly enhanced gamma-band response under physostigmine compared to placebo for right frontal cortex. This is also confirmed in timecourses **(H)** of induced 50-70Hz gamma for these two conditions. Values plotted are z-values for post-vs pre-stimulus power. Topography thresholded at $p<0.01$. Thus stimulus-induced gamma over right frontal cortex [45], a site implicated in the attentional control network, was influenced by physostigmine, in contrast with the unaffected gamma in visual cortex. This effect did not correlate significantly ($p > 0.1$) with behaviour or the attentional effects in visual cortex.

Partial correlation analysis on evoked subtracted data

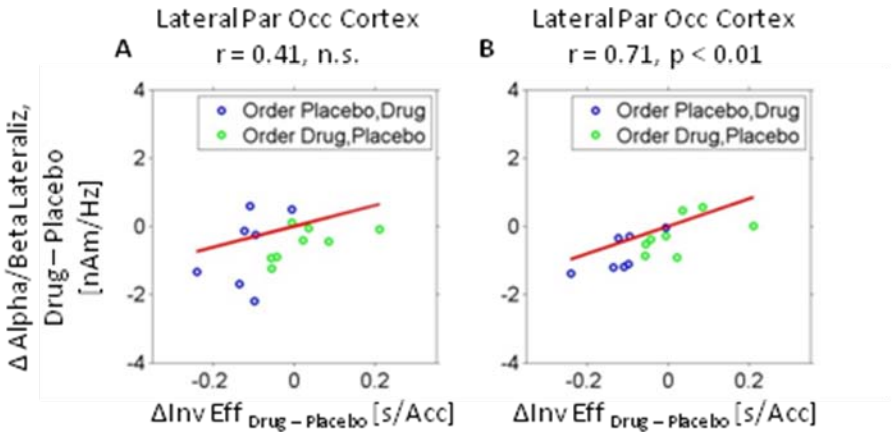

Figure S3 – Partial correlation analysis, **related to Figure 4**

These scatterplots are analogous to Figure 4 but depict the drug-modulation of the spatial attention effect after removal of drug effects on alpha-beta-power in the respective t-f-window (after the evoked field was removed). To remove the effect of the drug on alpha/beta-power a regression of the power values (collapsed over attentional conditions) on the drug effect on attentional difference was computed and the residual y-values were taken as the new attentional difference scores.

As in Figure 4, **(A)** shows the correlation with the lateral parts of parieto-occipital cortex (Fig.2F, 10-20Hz, 0-200ms). **(B)** shows the correlation with an ROI in the parieto-occipital sulcus (Supplemental figure S1), a structure tightly linked with alpha-oscillations at the t-f-window where the drug-effect is maximal there (5-15Hz, 0-350ms). Difference of attentional lateralization across drug and placebo condition (minus the drug effect on raw power) for right minus left hemispheres are shown on the y-axis, differences of inverse efficiency is shown on the x-axis. Each point gives difference scores for one participant, in blue the subjects where the drug session followed placebo and in green where drug preceded placebo. Negative values on the x- and y-axis indicate stronger effects in the expected direction (stronger hemispheric lateralization and faster processing for the physostigmine condition). Subjects for whom the drug was administered in the second session tend to have stronger effects.

Table S1: Centroid coordinates (MNI space)

	X (mm)	Y (mm)	Z (mm)
Beta Placebo centroid 1	34.06	-65.14	52.19
Beta Placebo centroid 2	33.21	-29.02	66.87
Beta Placebo centroid 3	41.68	-20.80	40.12
Beta Placebo centroid 4	61.29	-43.52	23.15
Beta Interaction lateral parieto occipital centroid 1	22.56	-64.16	43.16
Beta Interaction lateral parieto occipital centroid 2	28.41	-81.68	38.31
Beta Interaction lateral parieto occipital centroid 3	59.19	-52.45	-9.64
Alpha Interaction medial parieto-occipital centroid	19.43	-74.62	32.32
Gamma Placebo centroid 1	19.53	-82.80	-15.08
Gamma Placebo centroid 2	33.78	-33.09	-13.32
Gamma Placebo centroid 3	27.77	-43.58	67.63
Gamma Placebo centroid 4	31.80	-77.14	33.25
Gamma Placebo centroid 5	39.90	-66.38	-5.02

These centroids reflect the centers of gravity of local maxima of symmetrical attentional hemispheric lateralization – combined for left and right hemispheres for more robust estimates - and here the values are given for the right hemisphere.

Supplemental Experimental Procedures

Participants

Participants were recruited from an online data-base and gave informed consent prior to participation with the right to exit the study at any time. Exclusion criteria included: neurological disorders or family history of epilepsy; asthma or other strong allergy; cardiovascular disease; metabolic disease; glaucoma; influence of other drugs. Sixteen healthy male volunteers (mean age 25.6 years, s.d. 5.7 yrs) participated after informed consent in accord with ethical clearance. Females were not included as menstrual cycle may impact on drug sensitivity [35]. Participants trained on the task and then performed two MEG sessions, one under drug, one with placebo. These sessions were separated by at least two days, with order of drug or placebo counterbalanced across participants. Only the physician responsible for administering the agent/placebo knew whether it was placebo or drug, not the experimenter nor the participant.

Procedure and Drug administration

All participants underwent pre-training on the visual attention task (one or two sessions, until performance stabilized) with emphasis on maintaining central fixation and in order to determine the tilt-offsets yielding ~90% correct performance.

For the MEG sessions, participants were required not to drink alcohol the night before and no caffeine on the day of measurement. The responsible physician inserted the intravenous line before participants were brought to the magnetically shielded room (MSR). Participants then were sat comfortably in the MEG environment with peripheral electrodes (electrooculogram and electrocardiogram), head-localization coils and pulse-oxymeter attached. For drug sessions first 0.2mg Glycopyrrolate (a peripheral antidote to the cholinergic agonist Physostimgine that does not cross the blood-brain-barrier, see [10,11]) diluted in 5ml of saline was injected, while during

Placebo the same amount of pure saline was injected, via a 3-way port attached to the canule. The intravenous line was then attached to the pump (outside the MSR) and continuous infusion of either Physostigmine in a saline solution or else pure saline (Placebo) started at a rate titrated to individual bodyweight. Either 1 or 2mg Physostigmine was diluted in a 50 ml syringe filled with saline and the solution administered at a rate corresponding to 0.01 mg Physostigmine per kg bodyweight per hour (e.g. for a participant weighing 70 kg, 1ml Physostigmine was diluted in 50ml saline and infusion rate set to 35.7 ml solution per hour, corresponding to 0.7 mg Physostigmine per hour). Total infusion time was 70 min, starting 25 min prior to the experiment (to reach a more stable level of physostigmine plasma-levels, see [10,11]) then continuing for a further 45 min to limit the total dose given (see [46]). The experiment continued for another 15 min (half-time of Physostigmine plasma concentration is approximately 1-2 hours). In the 25 minutes prior to the experiment the seating position was optimised, the participant practised the task again and the head was localized. During the experiment heartbeat was continuously monitored via ECG and pulse-oxymetry. Placebo and drug sessions were separated by at least 2 days, in fully counterbalanced order.

Task

The task was to judge whether the grating on the attended side (as precued at trial start) was tilted clockwise or counterclockwise from diagonal. The grating in the currently unattended hemifield had an independent tilt (compared to the one in the attended hemifield) from diagonal but the global orientation of the gratings (top pointing to left or right) in the two hemifields was always opposite, to preclude any temptation of judging the grating presented in the irrelevant hemifield.

We used two cohorts of participants (n=8 each), each undergoing counterbalancing of drug/placebo order. In both cohorts the target tilt-offset during MEG sessions was initially chosen to yield ~90% correct performance as achieved during pre-training. In the first cohort we used a staircase

procedure during MEG, whereby < 75% correct performance over 24 trials would lead to an increase in the tilt-offset of 0.25 degrees, while >90% performance would lead to a corresponding reduction in tilt. This yielded actual mean tilt-offsets that did not differ between drug and placebo sessions (means 5.46 and 5.71 degrees for drug and placebo, respectively, s.d.s of 2.42 and 2.63 degrees). Since staircasing did not lead to significant drug/placebo differences in tilt-offset for the first cohort, for the second cohort this offset was kept constant, with its value again chosen to yield ~ 90% correct performance based on pre- training. MEG results were equivalent for the two cohorts, hence pooled.

Behavioural data analysis

We performed a regression analysis on the difference between drug and placebo in RT with drug/placebo session order as a covariate. Participants were faster in their second than first session (770.8 vs 828.3 ms); $t(15)=2.69$, $p<0.01$. They were faster under physostigmine than placebo (779.8 ms vs 819.2); $t(15)=-1.84$, $p<0.05$. The same outcomes were found if analyzing inverse-efficiency behavioral scores [36] instead, which combine RT and accuracy rate as RT divided by proportion correct ($t(15)=2.52$, $p<0.05$ for the drug effect, and $t(15)=3.6$, $p<0.01$ for the order effect).

MEG recording and analysis

Recordings

Data were recorded continuously from 274 axial gradiometers (1 of the SQUIDs from the sensor array over the head was defunct) plus 35 reference channels, using a CTF Omega whole head system at sampling rate of 600 Hz. Head position was measured via three coils, one placed at the

nasion and two attached to in-ear-tubes from the Etymotics system, see [3] at the beginning and end of each run.

Preprocessing

MEG data (3rd order axial gradiometer) were processed using FieldTrip http://www.fieldtrip.nl [40], being epoched and then checked for EOG-artefacts, muscle artefacts and amplitude-jumps using Fieldtrip partial artefact removal. The rejection threshold was set semi-automatically as described elsewhere [3]. Finally, whole trials were then visually inspected for any remaining artefacts, using Fieldtrip 'rejectvisual'. All artefact rejection was done blind to attention-condition (needed to be separate for drug condition as these were different sessions).

Forward-modelling

For source analysis, individual participants' T1 weighted MRI images were used to derive a mesh (8296 grid points) of the cortical surface and to calculate an individual forward model. Datasets were imported into SPM8 http://www.fil.ion.ucl.ac.uk/spm [42] for coregistration of MEG and MRI, segmentation and cortical mesh-calculation. We used the option of warping the canonical segmented MNI-brain onto the individual MRI to get a volume-conduction-model based on the approach proposed by [41]. This has been shown to provide comparable or sometimes even better source-analysis results than when individually segmented brains are used to calculate the volume-conductor model [47] and is a standard option in SPM8 [42]. It provides a homologous representation of the cortical sheet across participants allowing efficient grandaveraging and associated statistics.

The so derived head- and volume-conductor-models were then imported into FieldTrip (see http://www.fieldtrip.nl) and forward models were calculated with orientation fixed to the direction of the largest projected power (a standard option in fieldtrip 'sourceanalysis').

Source and frequency analysis

All main analyses were performed directly in source space (although we separately performed a sensor-level analysis with interpolated synthetic planar gradients, as in [3], that gave highly convergent results). The representation of the cortical sheet (as 8296 grid points) was downsampled (using 'reducepatch.m' in MATLAB), resulting in a representation of 413 grid points. This number only mildly exceeds the 274 sensors while being less than the 548 planar gradiometers (vertical and horizontal planar gradients) on which frequency analyses would otherwise have to be calculated [3]. For transformation into source-space, we used a time domain linear beamforming approach called linearly constrained minimum variance filtering [44]. In this approach a spatial filter (beamformer) is calculated from the covariance matrix of the sensor data and the leadfield according to the following formula:

$$\boldsymbol{w}(\boldsymbol{r}) = (\boldsymbol{h}(\boldsymbol{r})'(\boldsymbol{C}+\lambda\boldsymbol{I})^{-1}(\boldsymbol{h}(\boldsymbol{r}))^{-1}\boldsymbol{h}(\boldsymbol{r})'(\boldsymbol{C}+\lambda\boldsymbol{I})^{-1} \quad (1)$$

where **r** denotes the position-vector of the respective gridpoint, **h** is the leadfield matrix for a given point (orientation disregarded, but see below), **C** is the covariance matrix of the axial gradient sensor data, **I** is the identity matrix, λ is the regularization parameter and **w** is the resulting spatial filter (or beamformer) coefficient vector. In our analyses, lambda was set to half the mean of the diagonal of the cross-correlation matrix, a heuristic that yielded smooth sensor-topographies of the filter coefficients without signs of 'overfitting' in all participants. Instead of the inverse of the regularised covariance matrix, the Moore-Penrose pseudoinverse was taken, as standard in Fieldtrip. We calculated two sets of filters for each MEG dataset (i.e. each datafile), one for low-frequencies the other for high-frequencies (see below), irrespective of attentional condition or time-in-trial. This approach has been shown to give particularly robust spatial filters [48].

For *low-frequency analyses* (alpha/beta) the time-series of the (non-realigned axial gradiometer data) were baseline-corrected over the entire epoch then low-pass-filtered to 40 Hz with a sixth-order Butterworth filter and the covariance matrix computed across the entire trial. The nonrealigned axial gradiometer data were multiplied with these filter coefficients (i.e. linear projection), resulting in 413 time-series for each grid point (the orientation at each grid point was chosen along the dominant direction of the filter-coefficients for each dipolar orientation, again a standard option in the Fieldtrip 'sourceanalysis' routine). A wavelet analysis was run where a complex exponential of frequencies from 2.5 to 40 Hz in steps of 2.5 Hz was multiplied with a Hanning taper (rather than a Gaussian as in the classical Morlet wavelet), with length 3 cycles of the base frequency (e.g. 300 ms for 10 Hz) from -1s before gratings onset until 0.8s after grating onset. The use of a Hanning taper rather than the classical Gaussian enables shorter time-windows and reduces data losses at window edges otherwise caused by the longer window cycles needed for the Gaussian (the Hanning instead tapers to zero at edges).

For *high-frequency analyses* (gamma), covariance was calculated for bandpass-filtered data (40 – 150 Hz). Fixed time-windows were used with discrete prolate spherical slepian (DPSS) tapers to optimize smoothing in time and frequency domains and to suppress noise outside the time-frequency period of interest [49]. The window length was 200 ms for all frequencies (from 40 to 150 Hz in steps of 5 Hz) and we used 3 tapers (resulting in approx 10 Hz smoothing in the spectral domain) over the same time-window as for low-frequencies.

To obtain stimulus induced changes of oscillatory activity the spectra were baseline-corrected according to the following method: The baseline was calculated separately for each frequency and grid point at the time-window centered around 300ms prior to cue onset and then subtracted from the spectra of the peri-stimulus period. For each subject t-values were then obtained by dividing the

baseline-subtracted power values by the combined standard error of the mean of baseline and placebo. These t-values were then converted to z-values and averaged across subjects.

Removal of evoked fields:

To investigate whether some of the effects were driven by responses phase-locked to the stimulus ("evoked") we first calculated for each subject the frequency domain representation of the evoked field – by simply averaging the complex Fourier-coefficients (rather than the magnitude of these as resulting in the power-spectrum). These averaged complex Fourier spectra (for each time-, frequency-bin and grid point) were then subtracted from the single trial Fourier-spectra and then the power-spectrum was computed for each individual trial and then averaged for each subject. This approach is numerically equivalent to calculating the power spectrum of the (unfiltered) evoked field and subtracting this from individual trials power spectra but was simpler to accomplish in our analysis flow (see also [4] for a similar analysis).

Analysis of spatial attention effects

Main Effect of Attention (regardless of Drug)

To test for symmetrically lateralized spatial attention effects on visual cortex, we assessed effects that were present for Attend Left versus Right (and vice-versa) in corresponding regions of the right and left hemisphere. To this end we first calculated random effect paired t-tests on power-spectra for the contrast 'Attend_Left (L) minus Attend_Right (R)' according to the formula

$$t = \frac{mean_L - mean_R}{stdErrDiffMean_{L-R}} \quad (2)$$

where '$mean_L$' and '$mean_R$' refer to the average (across subjects) power-spectral-density-values for 'Attend_Left' and 'Attend_Right' conditions and '$stdErrDiffMean_{L-R}$' refers to the standard error of the difference of the means. After selecting time-frequency-windows where this difference (the main effect of spatial attention *pooled across drug and placebo conditions,* hence unbiased with

respect to any drug impact) was pronounced (in close agreement with the existing literature on spatial attention effects on oscillations, [1-6]), we then tested for the mirror symmetric modulation of oscillatory power by spatial attention. To this end grid-points were only retained if they showed a significant difference ($p < 0.05$) in the above contrast (equation 2) AND had a *corresponding grid point* on the other cortical hemisphere. Corresponding grid points were defined as those lying within a sphere of 17mm radius (close to the nearest-neighbour distance for the downsampled grids) at the mirror-symmetric position in the other hemisphere which showed a significant attention effect (according to equation 2) but of opposite sign to the first hemisphere. The mirror-symmetric position is defined as the position at the same y-, z-coordinates (MNI coordinate system: x-axis for left-right, y-axis for anterior-posterior and z-axis for ventral-dorsal direction), but with the opposite sign x-coordinate. Searching within a sphere was necessary since no exactly mirror-symmetrical grid-points arise in the downsampled representation of cortical gridpoints.

For the time-frequency images (as shown in figures 2 and 3 in the main paper) in order to combine effects from left and corresponding right hemisphere regions into one summary value, we performed the following calculation where $t_{RightHemisphere}$ and $t_{LeftHemisphere}$ refer to the result from equation 2 for the significant gridpoints from the right and left hemisphere, respectively:

$$t_{combined} = t_{RightHemisphere} - t_{LeftHemisphere} \qquad (3)$$

Statistical inference was then assessed by calculating the following test-statistic, averaging over time- (t), frequency- (f) and grid-points (s) of interest:

$$AttEff_{combined} = \sum_s^S \sum_t^T \sum_f^F ((AttL_{RightHem}(s,t,f) - AttR_{RightHem}(s,t,f)) - (AttL_{LeftHem}(s,t,f) - AttR_{LeftHem}(s,t,f)))/(F * T * S) \qquad (4)$$

where $AttL_{RightHem}(s,t,f)$ in equation 4 corresponds to the average power-spectral density of a right hemispheric grid point *s* at time-bin *t* and frequency bin *f* over trials where the left hemifield was

attended (and correspondingly $AttR_{LeftHem}(s,t,f)$ the average power-spectral-density of a left hemispheric grid point over trials where the right hemifield was attended.

This attentional lateralization index was then tested against zero with the following t-test:

$$t = \frac{Mean(AttEff_{combined}) - 0}{StdErrMean(AttEff_{combined})} \qquad (5)$$

$Mean(AttEff_{combined})$ denotes the average of the attentional lateralization index (equation 4) over subjects and $StdErrMean(AttEff_{combined})$ correspondingly the standard error of the mean of these values.

Drug modulation of attention effects

For assessing drug impacts on symmetric lateralized attention effects, we calculated the difference between attentional lateralization of power in Drug vs Placebo condition:

$$A_{DrugModulation} = [Att\_L - Att\_R]_{Drug} - [Att\_L - Att\_R]_{Placebo} \qquad (6)$$

and then assessed the significance of a deviation of this value (equation 6) again combined for the two hemispheres (in analogy to equation 4) against zero. This was performed in those regions-of-interest (time-frequency aspects of visual cortex) where we had already observed symmetric main effects of attention, regardless of the drug-manipulation (hence unbiased for the drug versus placebo contrast):

$$t_{DrugModulation} = \frac{Mean(A_{DrugModulation}) - 0}{StdErrMean(A_{DrugModulation})} \qquad (7)$$

t-values reported in the main text for drug impacts on attentional lateralization are the outcome of averaging power-spectral-densities in the same space-time-frequency-space region of interest as identified for the main-effects of attention (hence unbiased for potential drug-placebo difference) and then performing the new test for significance of the drug impact (equation 7).

For the effect shown in the parieto-occipital sulcus shown in Supplemental figure 1, a region of interest (ROI) was located in the left and right bank of the parieto-occipital sulcus and spatial

attention effects for this were then calculated in the same way as described above. We investigated this region more closely because of its known relevance as the key generator of alpha-oscillations in visual cortex and because previous studies have shown that cholinergic neuromodulation may impact on alpha-beta-oscillations there [26,27].

Estimation of centroids of attentional hemispheric lateralization results

In order to give meaningful coordinates of those brain regions significantly modulated by attention (or attention being significantly modulated by the drug) we developed a procedure as described below. This seemed necessary given the spatially extended nature of the observed attentional modulations – where mean coordinates of all significant grid points would not necessarily be very meaningful given the 3D folded nature of the brain.

We searched across the entire cortical representation for local maxima in the statistics for attentional differences. These local maxima were defined as those grid points that were only surrounded by neighbouring grid-points with lower absolute t-values. Then we calculated the (weighted) mean coordinates of all significantly modulated grid points within a sphere centered around the respective local maximum – weighted by their attentional modulation strength (t-value). To give more robust estimates of these centroids we collapsed the statistic across both hemispheres and report here the coordinates for locations in the right hemisphere.

Brain-behaviour relations

We calculated for each participant (and session, i.e. drug or placebo) their average for the same time-frequency windows as marked in the Results figures (fig. 2-3) of the main paper. We then correlated these participant-by-participant physiological effects, due to the causal drug intervention,

with the corresponding inverse-efficiency scores (as well as reaction time, not reported here), using Pearson correlation coefficients.

We further tested the specificity of these correlations by 1) repeating the analysis on evoked-field removed data and 2) partializing the drug effect on alpha/beta-power out from the attentional lateralizations. The results of this analysis are shown in Supplemental Figure S3.

Supplemental References

45. Apparsundaram, S., Martinez, V., Parikh, V., Kozak, R., Sarter, M. (2005) Increased capacity and density of choline transporters situated in synaptic membranes of the right medial prefrontal cortex of attentional task-performing rats. J. Neurosci. *25*, 3851-6

46. Bentley, P., Driver, J., Dolan, R.J. (2008) Cholinesterase inhibition modulates visual and attentional brain responses in Alzheimer's disease and health. Brain. *131*, 409-24.

47. Henson, R.N. , Mattout, J., Phillips, C., Friston, K.J. (2009) Selecting forward models for MEG source-reconstruction using model-evidence. Neuroimage *46*, 168-76.

48. Litvak, V., Eusebio, A., Jha, A., Oostenveld, R., Barnes, G.R., Penny, W.D., Zrinzo, L, Hariz, M.I., Limousin, P., Friston, K.J., Brown, P. (2010) Optimized beamforming for simultaneous MEG and intracranial local field potential recordings in deep brain stimulation patients. Neuroimage. *50*, 1578-88.

49. Mitra, P.P., Pesaran, B. (1999) Analysis of dynamic brain imaging data. J Biophys *76*, 691-708.